Int. J. Heat Mass Transfer. Vol. 24, No. 4, pp. 739–747, 1981
Printed in Great Britain

0017–9310/81/040739–09 $02.00/0

EFFECTS OF THERMAL WALL RESISTANCE ON THE STABILITY OF CONDUCTION REGIME IN AN INCLINED NARROW SLOT

M. A. HASSAB
Mechanical Engineering Department, Alexandria University, Alexandria, Egypt
and
M. N. ÖZIŞIK
Mechanical and Aerospace Engineering Daprtment, North Carolina State University, Raleigh, NC 27650, U.S.A.

(*Received* 15 *August* 1980 *and in revised form* 9 *October* 1980)

Abstract—The effects of thermal wall resistance on the onset of cellular convection motion in a fluid confined inside an inclined slot having a very large aspect ratio and subjected to convective boundary conditions are investigated analytically for the longitudinal and transverse rolls, and numerical calculations are performed for the case of $Pr = 0.72$. In order to establish the range of validity of the lumped parameter analysis used in some of the previous work on the effects of walls on stability criteria, the present results are compared with those obtained by the lumped parameter analysis. It is shown that, when the thermal conductivity and the thickness of the walls are about of the same order of magnitude or larger than those for the fluid, the results based on the lumped parameter analysis are unrealistic. The effects of walls on the transition angle for the cross over from the longitudinal to transverse rolls are investigated.

NOMENCLATURE

a,	dimensionless wave number;
d,	thickness of the fluid layer;
g,	gravitational acceleration;
Gr_e,	external Grashof number, $\gamma g(T_{\infty 1} - T_{\infty 2})d^3/\nu^2$;
h_1, h_2,	heat transfer coefficients;
H_1, H_2,	Biot numbers based on fluid conductivity, $H = h_i d/k$;
H_{w1}, H_{w2},	Biot numbers based on wall conductivities, $H_{wi} = h_i d/k_i$;
k,	thermal conductivity of fluid;
k_1, k_2,	thermal conductivity of the lower and upper wall;
L,	height of slot;
Pr,	Prandtl number, ν/α;
Ra_e,	external Rayleigh number, $\gamma g(T_{\infty 1} - T_{\infty 2})d^3/\alpha\nu$;
Ra,	internal Rayleigh number, $\gamma g[\bar{T}(0) - \bar{T}(d)]d^3/\alpha\nu$;
s_1, s_2,	lower and upper wall thickness ratios, t_i/d;
t_1, t_2,	lower and upper wall thicknesses;
t,	dimensionless time, $\nu\tau/d^2$;
T,	fluid temperature;
$T_{\infty 1}, T_{\infty 2}$,	environment temperatures at the lower and upper walls respectively;
v^*,	dimensionless perturbed velocity component in y-direction;
u_0,	characteristic velocity, $\gamma g(T_{\infty 1} - T_{\infty 2})d^2 \cdot \cos\delta/\nu$;
X, Y,	Cartesian coordinates with y measured normal to the walls;
x, y,	$= (X, Y)/d$.

Greek letters

α,	thermal diffusivity of the fluid;
α_1, α_2,	thermal diffusivities of lower and upper walls, respectively;
γ,	coefficient of thermal expansion for fluid;
γ_1, γ_2,	parameters defined as, α/α_i;
δ,	angle measured from horizontal;
δ_0,	transition angle;
θ^*,	dimensionless perturbed temperatures;
κ_{w1}, κ_{w2},	lower and upper walls conductivity ratios, k_i/k;
ν,	kinematic viscosity;
ψ,	dimensionless perturbed stream function;
τ,	time.

Superscripts

$\bar{}$,	mean quantities;
*,	refers to perturbed quantity.

Subscripts

∞,	refers to outside environment;
1, 2,	lower and upper wall respectively.

INTRODUCTION

THIS PAPER is concerned with the effects of the thermal resistances of the walls on the stability of natural flow in the conduction regime inside an inclined slot. In an earlier work on this subject, Ostroumov [1] evaluated the critical Rayleigh number for a viscous fluid heated from below inside an infinitely long circular cylinder with an infinitely thick wall in terms of the ratio of the

wall thermal conductivity to the fluid conductivity. The same problem was studied later by Slavnov [2] for the case of finite wall thickness. Other investigators [3–5] included the effects of convective boundary conditions but neglected the thermal resistance of the walls. The effect of wall thermal resistance on stability for the Bénard problem was studied by Hurle, Jackman and Pike [6] by assuming that the fluid was bounded by two solid walls of infinite extent and having identical finite thermal conductivity. Later on, Nield [7] considered a similar problem, but only for the case when the fluid was bounded below by a rigid wall of infinite conductivity and above by a solid wall of finite conductivity and finite thickness.

The stability of natural flow in a narrow vertical or inclined slot having walls kept at different isothermal temperatures has been examined [8–19] for all Prandtl numbers. These results confirm that instability occurs as either two-dimensional longitudinal rolls which are dominant in the range of angles of inclination $0 < \delta < \delta_0$, or as two-dimensional transverse rolls in the range $\delta_0 < \delta \leq 90$, where δ_0 is the transition angle (i.e. for transition from longitudinal to transverse rolls) measured from the horizontal. When transverse rolls have priority of occurrence over longitudinal rolls, instability sets in as stationary cells for $Pr < 12.7$ and in the form of travelling waves for $Pr > 12.7$.

It is apparent from the aforementioned survey of literature that the effects of the conductivity and the thickness of both walls on the stability of a fluid in an inclined slender slot, subjected to convective boundary conditions, have not yet been studied.

ANALYSIS

Consider a layer of fluid of thickness d, kinematic viscosity ν, thermal conductivity k, thermal diffusivity α, and coefficient of thermal expansion γ, contained in a narrow inclined slot. The lower surface of the fluid layer is bounded by a wall of finite thickness t_1 and conductivity k_1, while the upper surface is bounded by a solid wall of thickness t_2 and conductivity k_2. These walls are subjected to convective boundary conditions at their outer surfaces, such that, h_1 is the heat transfer coefficient at the lower surface and h_2 is the heat transfer coefficient at the upper one. If the environment temperatures $T_{\infty 1}$ and $T_{\infty 2}$, illustrated in Fig. 1, are such that $T_{\infty 1} > T_{\infty 2}$, a unicellular convective motion sets up so that fluid near the hot plate rises upwards and that near the cold plate flows downwards. If the temperature difference, $T_{\infty 1} - T_{\infty 2}$, is gradually increased, the initial laminar flow between the plates breaks up and a secondary flow sets up in the form of two dimensional multicellular convection. To investigate the conditions for the initiation of such an instability in the flow field, the linear perturbation theory is applied to the governing equations of motion and energy in the Boussinesq approximation. After eliminating the pressure, the resulting differential equations governing the formation of the longitudinal and transverse rolls are given in the dimensionless form.

Equations for the longitudinal rolls

$$\left[\frac{\partial}{\partial t} - (D^2 - a_2^2)\right](D^2 - a_2^2)v^* = -a_2^2\theta^* \cos\delta \qquad 0 < y < 1 \quad (1a)$$

$$\left[Pr\frac{\partial}{\partial t} - (D^2 - a_2^2)\right]\theta^* + Ra_e D\bar{\theta}v^* = 0 \qquad 0 < y < 1 \quad (1b)$$

Equations for the transverse rolls

$$\left[\frac{\partial}{\partial t} - (D^2 - a_1^2)\right](D^2 - a_1^2)v^* + ia_1 Gr_e \sin\delta[\bar{U}_v(D^2 - a_1^2) - D^2\bar{U}_v]v^* = -(a_1^2\theta^* \cos\delta + ia_1 D\theta^* \sin\delta) \quad (2a)$$

$$\left[Pr\frac{\partial}{\partial t} - (D^2 - a_1^2)\right]\theta^* + ia_1 Ra_e\bar{U}_v\theta^* \sin\delta + Ra_e D\bar{\theta}v^* = 0. \quad (2b)$$

Equations for the lower and upper walls

$$\left[Pr\gamma_1\frac{\partial}{\partial t} - (D^2 - a_i^2)\right]\theta_1^* = 0 \quad 0 < y < -s_1 \quad (3a)$$

$$\left[Pr\gamma_2\frac{\partial}{\partial t} - (D^2 - a_i^2)\right]\theta_2^* = 0 \quad 1 < y < 1 + s_2 \quad (3b)$$

where $\gamma_i = \alpha/\alpha_i$, $i = 1.2$, is the diffusivity ratio, a_1 is the wave number for the transverse rolls and a_2 for the longitudinal rolls in the x- and z-directions respectively. It is to be noted that the Prandtl number, Pr, appearing in the equations for the walls results from the fact that the dimensionless time is defined as $t = \tau\nu/d^2$, where τ is the dimensional time. The boundary conditions for the above equations are taken, for the case of rigid walls as

$$v^* = Dv^* = 0 \qquad \text{at } y = 0, 1 \quad (4a)$$

$$\theta^* = \theta_1^*, \quad D\theta^* = \kappa_{w1}D\theta_1^* \qquad \text{at } y = 0 \quad (4b)$$

$$\theta^* = \theta_2, \quad D\theta^* = \kappa_{w2}D\theta_2^* \qquad \text{at } y = 1 \quad (4c)$$

$$D\theta_1^* - H_{w1}\theta_1^* = 0 \qquad \text{at } y = -S_1 \quad (4d)$$

$$D\theta_2^* + H_{w2}\theta_2^* = 0 \qquad \text{at } y = 1 + S_2 \quad (4e)$$

where $D \equiv \partial/\partial y$; v^* is the dimensionless component of the perturbed velocity normal to the plates; θ^*, θ_1^*, and θ_2^* are the perturbed temperatures in the fluid, and in the lower and upper plates, respectively; and x and y are the dimensionless coordinates parallel to and normal to the walls. In addition, S_1 and S_2 are the dimensionless thicknesses of the lower and upper walls; Gr_e and Ra_e are the external Grashof and Rayleigh numbers which are defined on the basis of the difference between the temperatures $T_{\infty 1}$ and $T_{\infty 2}$ of

the environments. H_{w1} and H_{w2} are the Biot numbers for the lower and upper walls based on the conductivity of the walls respectively; κ_{w1} and κ_{w2} are the conductivity ratios of the lower and upper plates respectively; γ_1 and γ_2 are the diffusivity ratios of the lower and upper plates and δ is the angle of inclination measured from horizontal. In equations (3), the subscript $i = 1$ stands for transverse waves and $i = 2$ for the longitudinal waves. The quantities $\bar{U}_v$ and $D\bar{\theta}$ refer to the dimensionless base flow velocity component in the x-direction and the base flow temperature respectively. They are determined from the base flow analysis in the conduction regime as

$$\bar{U}_v = \frac{1}{12} y(1-y)(1-2y);$$

$$D\bar{\theta} = -\frac{1}{1 + \left[\frac{1}{H_1} + \frac{s_1}{\kappa_{w1}}\right] + \left[\frac{1}{H_2} + \frac{s_2}{\kappa_{w2}}\right]} \quad (5)$$

where $H_i = h_i d/k$, $i = 1, 2$.

The analysis for longitudinal rolls

It can be shown by the principle of exchange of stabilities that, in the case of longitudinal waves defined by equations (1), (3) and (4), the instability sets in as stationary cells, not as overstability. This matter is discussed in the Appendix. When the longitudinal rolls have priority of occurrence over transverse rolls, the free convection occurs in the form of stationary rolls and one can set $\partial/\partial t = 0$ in the analysis of stability.

The solutions of equations (3) subject to the conditions (4d) and (4e) are taken as

$$\theta_1^* = A[a_2 \cosh a_2(s_1 + y) + H_{w1} \sinh a_2(s_1 + y)] \quad (6a)$$

$$\theta_2^* = B[a_2 \cosh a_2(1 + s_2 - y) + H_{w2} \sinh a_2(1 + s_2 - y)] \quad (6b)$$

where A and B are constants.

Conditions (4b) with equation (6a) give

$$\frac{1}{\theta^*} D\theta^* = \kappa_{w1} \frac{1}{\theta_1^*} D\theta_1^* = \xi_1$$

or

$$D\theta^* - \xi_1 \theta^* = 0 \quad \text{at } y = 0. \quad (7a)$$

Similarly, the conditions at $y = 1$ is

$$D\theta^* + \xi_2 \theta^* = 0 \quad \text{at } y = 1 \quad (7b)$$

where

$$\xi_i = \kappa_{wi} a_2 \left[\frac{H_{wi} + a_2 \tanh a_2 s_i}{H_{wi} \tanh a_2 s_i + a_2}\right], \quad i = 1, 2. \quad (7c)$$

Now, by setting $\partial/\partial t = 0$, equations (1) reduce to

$$(D^2 - a_2^2)^2 v^* = a_2^2 \theta^* \cos\delta \quad (8a)$$

$$(D^2 - a_2^2)\theta^* = Ra_e D\bar{\theta} v^* \quad (8b)$$

and the boundary conditions (4d) and (7a, b), for the case of 'two rigid walls' are written as

$$v^* = Dv^* = D\theta^* - \xi_1 \theta^* = 0 \quad \text{at } y = 0 \quad (9a)$$

$$v^* = Dv^* = D\theta^* + \xi_2 \theta^* = 0 \quad \text{at } y = 1. \quad (9b)$$

For the case of *'lower wall rigid and upper one free'*, which is applicable for the horizontal position, the above differential equations (8) and the boundary conditions (9a) at the lower rigid wall are still applicable; but the hydrodynamic and thermal boundary conditions at the upper surface will be replaced by

$$v^* = D^2 v^* = D\theta^* + H_2 \theta^* = 0 \quad \text{at } y = 1. \quad (9c)$$

The solution for longitudinal rolls. The above eigenvalue problem for the longitudinal rolls is solved by the application of the *Chadrasekhar Method* for the cases of 'two rigid walls' and 'lower wall rigid, upper surface free', because this method converges very fast and gives quite accurate results in few approximations [20] with this type of problem. To perform the analysis, the function $v^*(y)$ is represented in a series of orthogonal functions Φ_m in the form

$$v^*(y) = \sum_{m=1}^{\infty} A_m \Phi_m(y) \quad (10a)$$

where, the orthogonal function $\Phi_m(y)$ are taken as [20]

$$\Phi_m(y) = \frac{\cosh \alpha_m y - \cos \alpha_m y}{\cosh \alpha_m - \cos \alpha_m} - \frac{\sinh \alpha_m y - \sin \alpha_m y}{\sinh \alpha_m - \sin \alpha_m}. \quad (10b)$$

The auxiliary eigenvalues α_ms are the roots of the transcendental equation

$$\cosh \alpha \cos \alpha = 1 \quad \text{(both walls rigid)} \quad (11a)$$

$$\coth \alpha - \cot \alpha = 0 \quad \text{(lower wall rigid, upper one free).} \quad (11b)$$

The above solution (10) for v^* is introduced into equation (8b), and the resulting equation is solved to determine θ^* analytically. The approximate solutions thus obtained for v^* and θ^* are then introduced into

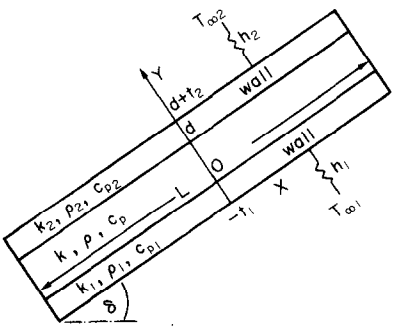

Fig. 1. Cross-section of the physical problem.

equation (8a) and the orthogonality conditions of the Φ_m functions are utilized to obtain a set of infinite algebraic homogeneous equations. By truncating these equations after N terms, the resultant set yields an $N \times N$ secular determinant for the determination of the external Rayleigh number Ra_e.

$$\| a_{mn} + a_2^2(Ra_e \cos\delta)b_{mn} \| = 0 \tag{12}$$

where

$$a_{mn} = \int_0^1 (D^2 - a_2^2)^2 \Phi_m(y)\Phi_n(y)\,dy \tag{13a}$$

$$b_{mn} = \int_0^1 D\bar{\theta} \cdot \theta_m(y) \cdot \Phi_n(y)\,dy. \tag{13b}$$

Here in equations (13) the two integrals are performed analytically. Once these integrals are known, the external Rayleigh number, Ra_e, is computed by satisfying equation (12) for different values of the wave number 'a_2' with each fixed system of input parameters 'H_1, H_2, κ_{w1}, κ_{w2}, S_1, S_2'. The minimum of these Rayleigh numbers for each system of input parameters establishes the critical Rayleigh number, marking the conditions for the onset of instability associated with the occurrence of longitudinal vortex rolls.

The analysis for transverse rolls

The stability problem associated with the transverse rolls are governed by the differential equations (2) and (3) and the boundary conditions (4). We note that the equations (2) are complex, as a result their solutions v^* and θ^* are complex functions. The wall equations (3) and their boundary conditions (4d,e) at the outer boundaries are real, but at the inner boundaries the boundary conditions (4b,c) are coupled to the fluid temperature θ^*, which is complex. Therefore, the solution for the wall temperatures is expected to be complex.

We assume a disturbance in the form

$$[\psi^*(y,t),\ \theta^*(y,t)] = [\psi(y),\ \theta(y)]e^{ct} \tag{14}$$

and introduce this result into equations (2)–(4), and follow a procedure described previously. The thermal boundary conditions at the interior surfaces become

$$D\theta \mp \lambda_i\theta = 0 \quad \text{at } y = 0,1 \tag{15a}$$

where

$$\lambda_i = \kappa_{wi}b\left[\frac{H_{wi} + b\tanh bs_i}{H_{wi}\tanh bs_i + b}\right], \quad i = 1,2 \tag{15b}$$

and

$$b = [a_1^4 + (\gamma_i Prc)^2]^{1/4}\, e^{i\eta/2}$$

$$\eta = \tan^{-1}\left(\frac{\gamma_i Prc}{a_1^2}\right).$$

Here, the parameter c is in general a complex number, therefore the coefficients λ_i ($i = 1,2$) are complex too. For the case when the stability sets in as stationary cells, we have $c = 0$. Then the expression for λ_i becomes real and similar to the parameter ξ_i which previously appeared in equation (7c) for the longitudinal rolls.

It is apparent from equation (15b) that the wall parameters κ_{wi} and s_i affect the coefficients λ_i which in turn affect the onset of stability. For the limiting case, $\kappa_{wi} \to \infty$ (or $\lambda_i \to \infty$), that is when both boundaries are perfectly conducting, the analysis reduces to the one discussed in references [8–19] in which the transition Prandtl number (i.e. the value of the Prandtl number at which change over from the stationary cells to the travelling waves) has the value $Pr_t = 12.7$. For the other limiting case, $\kappa_{wi} \to 0$ (or $\lambda_i \to 0$), which corresponds to the nonconducting walls, the transition Prandtl number has the value $Pr_t = 0.95$ [21]. Therefore, for the intermediate cases of finite wall conductivity and finite wall thickness, the transition Prandtl number should lie between the above two limits, that is, $0.95 < Pr_t < 12.7$. No experimental data are available for the value of the transition Prandtl number for the cases when the wall conductivities are of the same order of magnitude as the fluid conductivity and with convective boundary conditions. Therefore, based on the arguments given above, so long as $Pr < 0.95$, it is expected that the transition from the conduction regime to the multicellular regime, for the case of transverse waves should occur in the form of stationary convective cells.

Therefore, by restricting the present analysis for fluids having Prandtl number $Pr < 0.95$, the equations governing the transverse waves are obtained from equations (2)–(3), by setting $\partial/\partial t = 0$ and replacing the velocity v^* by the stream function ψ^* (i.e. $\psi^* = iv^*/a_1$). We obtain

$$(D - a_1)^2\psi^* - ia_1 Gr_e \times \sin\delta[\bar{U}_v(D^2 - a_1^2)\psi^* - D^2\bar{U}_v\psi^*] = [ia_1\theta^*\cos\delta - D\theta^*\sin\delta] \tag{16a}$$

$$(D^2 - a_1^2)\theta^* - ia_1 Ra_e[\bar{U}_v\theta^*\sin\delta - D\bar{\theta}\psi^*] = 0 \tag{16b}$$

$$\psi^* = D\psi^* = D\theta^* \mp \lambda_i\theta^* = 0 \quad \text{at } y = 0,1 \tag{17}$$

where, the real parameter λ_i is obtained from equation (15b) by setting $c = 0$.

$$\lambda_i = \kappa_{wi}a_1\left[\frac{H_{wi} + a_1\tanh a_1 s_i}{H_{wi}\tanh a_1 s_i + a_1}\right]. \tag{18}$$

The solution for the transverse rolls. The above system of equations for the transverse rolls is solved by the Galerkin method which has been applied successfully in the problems of hydrodynamic stability [11, 17–19]. In this method, the functions ψ^* and θ^* are represented in the form of orthogonal infinite series. The orthogonal functions are so chosen as to satisfy the boundary conditions for the problem. These expansions are taken in the form [20]

$$\psi^* = \sum_{m=1}^{\infty} A_m\Phi_{2m-1}(y) + i\sum_{m=1}^{\infty} B_m\Phi_{2m}(y) \tag{19a}$$

$$\theta^* = \sum_{m=1}^{\infty} C_m \theta_{2n}(y) + i \sum_{m=1}^{\infty} D_m \theta_{2m-1}(y). \quad (19b)$$

The orthogonal functions Φ_m and the eigenvalues associated with them are given by equations (10b) and (11b) respectively. The orthogonal functions $\theta_m(y)$ and the eigenvalues associated with them are taken as

$$\theta_m(y) = \beta_m \cos \beta_m y + \lambda_1 \sin \beta_m y \quad (20a)$$

$$\tan \beta = \frac{\beta(\lambda_1 + \lambda_2)}{\beta^2 - \lambda_1 \lambda_2}. \quad (20b)$$

The coefficients A_m, B_m, C_m and D_m appearing in equations (19) are unknown constants. Substituting the expansions given by equations (19) into equations (16), equating the real and imaginary parts on both sides of each equation, and orthogonalizing, one obtains an infinite set of linear algebraic homogeneous equations. If these expansions are truncated after N terms the resultant set yields $4N$ equations for the $4N$ unknowns. The nontrivial solution of this system is characterized by the condition of the vanishing of the determinant which is written in the matrix form as

$$\|H_{mn}\| = 0 \quad \text{for } n = 1, 2, 3, \ldots \quad (21)$$

where the elements H_{mn} are real matrices of order $4N \times 4N$ resulting from the orthogonalization.

We investigated the effects of various system parameters, such as H_i, κ_{wi}, s_i, $i = 1$ or 2, on the critical Grashof number for the transverse rolls for $Pr = 0.72$. The value of $Gr_c \cong 8000$ at the vertical position for $\kappa_{wi} = \infty$ changes only slightly with these parameters and the inclination in the range where the transverse rolls were dominant [21].

RESULTS AND DISCUSSION

We now present the effects of the wall thickness ratios s_1 and s_2, the wall conductivity ratios κ_{w1} and κ_{w2} and the Biot numbers H_{w1} and H_{w2} for the lower and upper surfaces respectively, on the initiation of convective motion characterized by the critical internal Rayleigh number Ra_c. The internal Rayleigh number, Ra is defined on the basis of the difference between the base flow temperatures at the inner surfaces as

$$Ra = \frac{\gamma g[\bar{T}(0) - \bar{T}(d)]d^3}{\alpha \nu} \quad (22)$$

where $\bar{T}(0)$ and $\bar{T}(d)$ are the base flow temperatures at the inner surfaces of the lower and upper plates respectively. The *external Rayleigh number*, Ra_e, is defined on the basis of the difference between the outside temperatures, $T_{\infty 1} - T_{\infty 2}$, as

$$Ra_e = \frac{\gamma g(T_{\infty 1} - T_{\infty 2})d^3}{\alpha \nu}. \quad (23)$$

Then the relation between Ra and Ra_e is given by

$$Ra = \left[\frac{\bar{T}(0) - \bar{T}(d)}{T_{\infty 1} - T_{\infty 2}}\right] \cdot Ra_e \quad (24)$$

where

$$\frac{\bar{T}(0) - \bar{T}(d)}{T_{\infty 1} - T_{\infty 2}} = (-D\bar{\theta}). \quad (25)$$

Here, $(D\bar{\theta})$ is the base flow temperature gradient given in equation (5). In this analysis, we prefer to present the results in terms of the *critical internal Rayleigh number*, Ra_c, and the Biot numbers based on the thermal conductivity of the fluid (i.e. $H_i = h_i d/k$, $i = 1, 2$) in order to facilitate the comparison of the results with those in which the wall effects were neglected [3–5].

The convergence. The convergence of the solution for the analysis of the longitudinal rolls, for which the Chandrasekhar method was used, was found to be very fast; the difference between the third and the fourth approximations was less than 0.5%. The calculations performed for the transverse rolls are for $Pr = 0.72$ for all possible values of the input parameters H_i, κ_{wi} and s_i, with $i = 1, 2$. The results of calculations performed for the transverse rolls using 16×16 and 12×12 determinants was less than 0.3% for $Pr = 0.72$.

The transition angle. Calculations are performed for $Pr = 0.72$ to investigate the effects of the Biot number, the conductivity ratio and the thickness ratio for the lower and upper walls on the transition angle δ_0, that is the angle at which cross over takes place from the longitudinal to transverse rolls. Table 1 shows the variation of the transition angle δ_0 with identical values of the Biot numbers $H_1 = H_2$, the conductivity ratio $\kappa_{w1} = \kappa_{w2}$ and the wall thickness ratio $s_1 = s_2$ for the lower and upper walls for $Pr = 0.72$. For all the cases shown in this table, the transition angle, δ_0, increases with decreasing value of the wall conductivity ratio. The value of the transition angle $\delta_0 = 71.6$ for the case of $H_1 = H_2 \to \infty$ and $\kappa_{w1} = \kappa_{w2} \geq 100$ is in good agreement with that reported by Korpela [18] for the Bénard type problem in which the two surfaces of the fluid layer are kept at constant temperatures.

The variation of the wall thickness ratio, $s_1 = s_2$, appears to have an intriguing effect on the transition angle, δ_0, depending on the values of $H_1 = H_2$ and $\kappa_{w1} = \kappa_{w2}$. For example, for $H_1 = H_2 \to \infty$, the transition angle, δ_0, increases as the conductivity ratio decreases or the wall thickness ratio *increases*. On the other hand for $H_1 = H_2 = 0.01$, the transition angle, δ_0, increases as the conductivity ratio decreases or the wall thickness ratio *decreases*, excluding the case $\kappa_{w1} = \kappa_{w2} = 0.01$. For the case of $H_1 = H_2 = 1$, however, the transition angle may increase or decrease with the wall thickness ratio depending on the value of $\kappa_{w1} = \kappa_{w2}$. For example, the transition angle increases with increasing wall thickness ($s_1 = s_2$) for $\kappa_{w1} = \kappa_{w2} = 0.01$, whereas it decreases with increasing $s_1 = s_2$ for $\kappa_{w1} = \kappa_{w2} = 100$. The following discussion of the stability criteria will be helpful in the explanation of this phenomenon.

Table 1. The effects of H, κ_w and s on the transition angle δ_0 in degrees, measured from the horizontal, for $Pr = 0.72$

$H_1 = H_2 \to \infty$				
	$s_1 = s_2$			
$\kappa_{w1} = \kappa_{w2}$	0.01	0.1	1	≥ 2
0.01	78.2	80.97	81.86	81.98
0.1	73.73	78.18	80.57	80.70
1	71.86	73.68	76.37	76.40
10	71.60	71.85	72.45	72.45
≥ 100	71.60	71.60	71.60	71.60
$H_1 = H_2 = 1$				
	$s_1 = s_2$			
$\kappa_{w1} = \kappa_{w2}$	0.01	0.1	1	≥ 2
0.01	79.1	80.92	81.88	81.98
0.1	78.3	79.00	80.50	80.70
1	78.17	77.75	76.54	76.40
10	77.60	74.83	72.57	72.45
100	74.80	72.16	71.70	71.60
$H_1 = H_2 = 0.01$				
	$s_1 = s_2$			
$\kappa_{w1} = \kappa_{w2}$	0.01	0.1	1	≥ 2
0.01	81.92	81.93	81.96	81.98
0.1	81.89	81.75	80.88	80.69
1	81.75	80.47	76.75	76.40
10	80.46	75.36	72.58	72.45
100	75.33	72.17	71.70	71.70

The stability criteria for longitudinal rolls with both walls rigid

Figure 2 shows the effects of the wall thickness ratios s_1 and s_2 of the lower and upper walls respectively on the *critical internal Rayleigh number*, Ra_c, for various values of identical conductivity ratios (i.e. $\kappa_{w1} = \kappa_{w2}$) and for the case of $H_1 = H_2 \to \infty$ (i.e. the temperature at the outer surface of each wall is constant). This figure shows that, as the wall thicknesses are decreased or the wall conductivities are increased the flow is more stable. This can be explained qualitatively as follows: increasing the wall thickness or decreasing the wall conductivity reduces the heat dissipation through the walls. As a result the amplitude of the perturbed temperature in the fluid is amplified which in turn destabilizes the fluid. A more quantitative explanation of this matter can be given by referring to the boundary conditions given by equations (7a) and (7b) and the definition of the parameter ξ_i given by equation (7c). In these boundary conditions the parameter ξ_i appears as an effective Biot number. Then, as ξ_i is increased the heat dissipation through the walls is increased and as a result the stability is improved. For the case of $H_{wi} \to \infty$, equation (7c) reduces to

$$\xi_i = \frac{\kappa_{wi} a_2}{\tanh a_2 s_i}. \tag{26}$$

This result implies that, increasing κ_{wi} increases ξ_i, hence improves the stability. On the other hand, increasing s_i decreases ξ_i, which in turn decreases the stability.

The lumped parameter analysis has also been used in the literature [3–5] to investigate the effects of walls on the stability criteria. In order to establish the range of validity of the lumped parameter analysis, we lumped the thermal resistances of the walls and the outside surrounding according to the formulae

$$H_1^+ = 1\Big/\left(\frac{1}{H_1} + \frac{s_1}{\kappa_{w1}}\right), \quad H_2^+ = 1\Big/\left(\frac{1}{H_2} + \frac{s_2}{\kappa_{w2}}\right) \tag{27}$$

and for these values of H_1^+ and H_2^+ computed the critical internal Rayleigh number from corresponding analysis of the longitudinal rolls in reference [5]. The Ra_c obtained in this manner are compared with those in Fig. 2 for $H_1 = H_2 \to \infty$. The results of this comparison are listed in Table 2 for few cases. This table shows the deviation between the two critical Rayleigh numbers increases with the increasing values of the conductivity and wall thickness ratios considered in this example.

As a result, the lumped system can be used as a good criteria to evaluate the critical Rayleigh number, Ra_c, only for small wall conductivity ratios and small wall thickness ratios.

We also note from Fig. 2 that the limiting case, with $\kappa_{w1} = \kappa_{w2} \to \infty$, for any values of the wall thicknesses corresponds to the Bénard case, $Ra_c \cdot \cos\delta = 1708$.

Figures 3(a) and (b) have been prepared to show the variations of the critical internal Rayleigh number, Ra_c, with the Biot numbers H_1 and H_2 for different values of identical wall thickness ratios. The first of these is for $\kappa_{w1} = \kappa_{w2} = 1$ and the second for $\kappa_{w1} = \kappa_{w2} = 10$ and 100. It is apparent from both of these figures that increasing Biot numbers have a stabilizing effect on the fluid as previously discussed in references [3–5]. However, it is not so easy to draw a general conclusion on the effects of the wall thickness ratios s_1 and s_2 on the stability criteria merely by the inspection of the results presented in this figure. Therefore, we refer to the definition of ξ_i given by equation (7c) and examine the following three cases

(a) H_{w1} (or H_i) $\to 0$: equation (7c) reduces to

$$\xi_i = \kappa_{wi} a_2 \tanh(a_2 s_i). \tag{28a}$$

The, ξ_i increases with as κ_{wi} or s_i increases, as a result, the onset of instability is delayed as s_i or κ_{wi} is increased.

(b) $H_{wi} = a_2$: equation (7c) becomes

$$\xi_i = \kappa_{wi} a_2. \tag{28b}$$

This result means that ξ_i increases with κ_{wi}, but the wall thickness has no effect on the stability criteria for $H_{wi} = a_2$.

(c) $H_{wi} \to \infty$: the wall thickness has a stabilizing effect as shown in equation (26).

To illustrate the range of validity of the lumped

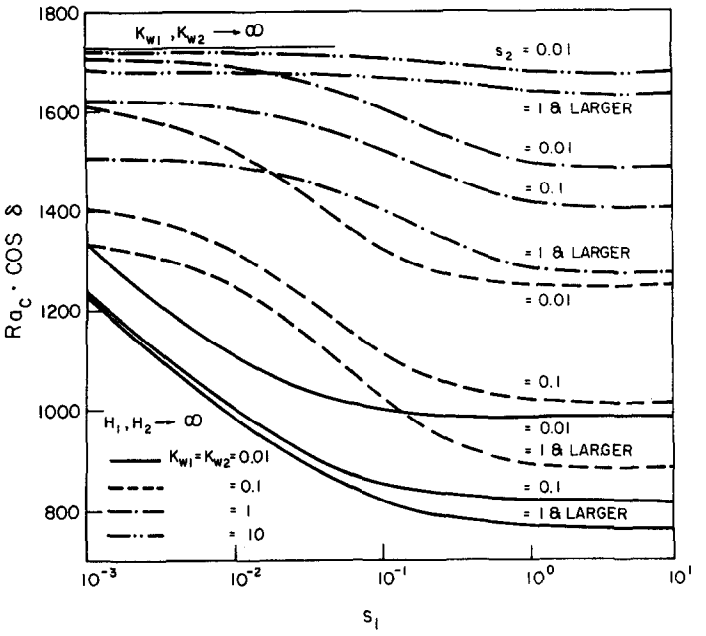

FIG. 2. Effects of the lower and upper wall thickness ratios s_1 and s_2, conductivity ratios κ_{w1} and κ_{w2} on the critical internal Rayleigh number Ra_c.

Table 2. Comparison between Ra_c computed from the present analysis and $(Ra_c)_{lump}$ for the lumped system

	$\kappa_{w1} = \kappa_{w2} = 0.1$		$\kappa_{w1} = \kappa_{w2} = 1$		$\kappa_{w1} = \kappa_{w2} = 10$	
$s_1 = s_2$	Ra_c	$(Ra_c)_{lump}$	Ra_c	$(Ra_c)_{lump}$	Ra_c	$(Ra_c)_{lump}$
0.01	1524	1511	1693	1681	1707	1705
0.01	1113	1100	1528	1511	1705	1681
1	891	845	1282	1100	1640	1511
10	879	858	1278	845	1639	1100

Table 3. The effects of the Biot numbers H_1 and H_2 on the differences between Ra_c computed from the present analysis and $(Ra_c)_{lump}$ for various identical values of wall conductivity ratios and wall thickness ratios

	$\kappa_{w1} = \kappa_{w2} = 0.1$				$\kappa_{w1} = \kappa_{w2} = 1$				$\kappa_{w1} = \kappa_{w2} = 10$			
	$s_1 = s_2 = 0.1$		$s_1 = s_2 = 1$		$s_1 = s_2 = 0.1$		$s_1 = s_2 = 1$		$s_1 = s_2 = 0.1$		$s_1 = s_2 = 1$	
$H_1 = H_2$	Ra_c	$(Ra_c)_{lump}$	Ra_c	$(Ra_c)_{lump}$	Ra_c	$(Ra_c)_{lump}$	Ra_c	$(Ra_c)_{lump}$	Ra_c	$(Ra_c)_{lump}$	Ra_c	$(Ra_c)_{lump}$
100	1191	1100	900	845	1566	1500	1309	1100	1678	1660	1647	1560
1	1033	997	895	835	1154	1090	1266	997	1423	1100	1630	1080
0.01	780	759	861	765	900	759	1246	759	1374	809	1629	760

parameter analysis of the wall effects on the stability criteria with the walls subjected to convective boundary conditions as considered in references [3–5], we present in Table 3 a comparison of the critical internal Rayleigh number, Ra_c, obtained from the present analysis and that determined by the lumped parameter analysis, $(Ra_c)_{lump}$. The results presented in this table indicate that when both the conductivity and thickness of the walls are about of the same order of magnitude or larger than those for the fluid, the results based on the lumped parameter analysis are unrealistic. Therefore, the validity of such results should be restricted to small thickness ratios of the walls (i.e. $t_i \ll d, i = 1,2$) with wall conductivities of the same order of magnitude or lower than the fluid conductivity.

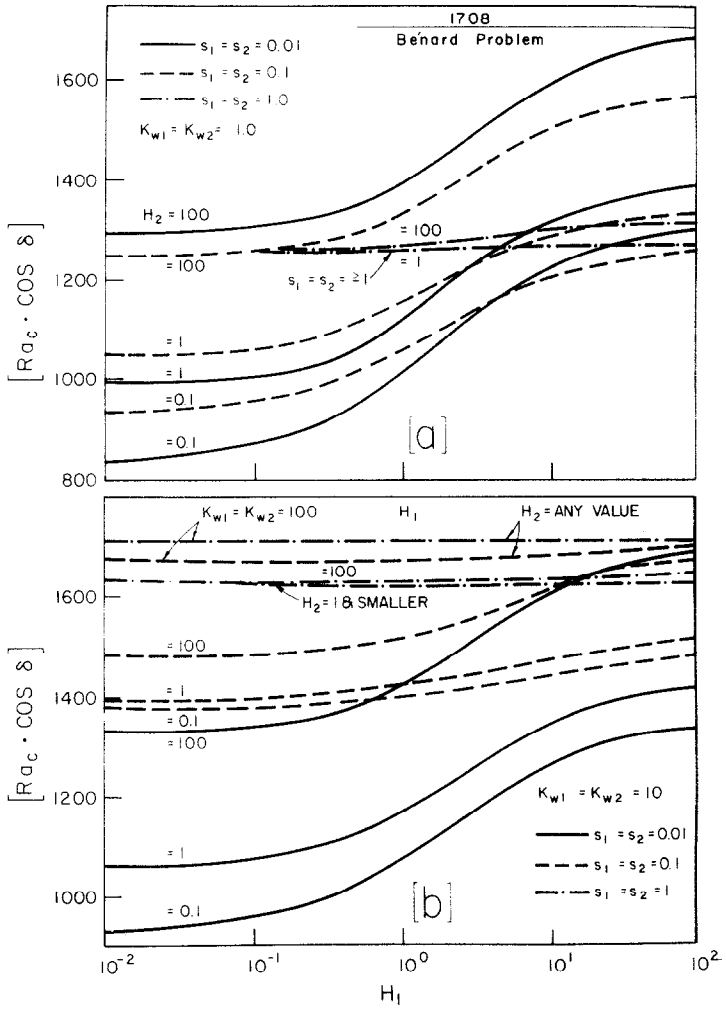

FIG. 3. Effects of wall parameters (s_1, s_2, κ_{w1}, κ_{w2}) and H_1, H_2 on Ra_c.

REFERENCES

1. G. A. Ostroumov, Free convection under conditions of the internal problem. *NACA Tech. Memo* 1407, 1958 (Translation of Convectzia V. Ousloviakh Vnoutrennia Zadachi, 1952).
2. V. V. Slavnov, Free convection in metallic vertical tubes of circular section, *Zh. Takh. Fiz.* **26**(9), 1938–1940 (1956).
3. E. M. Sparrow, R. J. Goldstein and V. K. Jonsson, Thermal instability in a horizontal fluid layer: effect of boundary conditions and non-linear temperature profile. *J. Fluid Mech.* **18,** 513–528 (1964).
4. E. M. Sparrow, L. Lee and N. Shamsundar, Convective instability in a melt layer heated from below, *J. Heat Transfer* **98c,** 88–94 (1976).
5. M. A. Hassab and M. N. Özişik, Stability of a layer of fluid subjected to convective boundary conditions, *Int. J. Heat Mass Transfer* **21,** 1264–1266 (1978).
6. D. T. J. Hurle, E. Jackman and E. R. Pike, On the solution of the Bénard problem with boundaries of finite conductivity, *Proc. Roy. Soc.* **A296,** 469–475 (1976).
7. D. A. Nield, The Rayleigh–Jeffreys problem with boundary slab of finite conductivity, *J. Fluid Mech.* **33,** 393–398 (1968).
8. G. Z. Gershuni, Stability of plane convective motion of a liquid, *Zh. Tech. Fiz.* **23,** 1838–1844 (1953).
9. R. N. Rudakov, On small perturbation of convective motion between vertical parallel walls, *P.M.M.* **30**(2), 439–445 (1967).
10. R. N. Rudakov, Spectrum of perturbations of stability of convective motion between vertical planes, *P.M.M.* **31**(2), 349–355 (1967).
11. C. M. Vest and V. S. Arpaci, Stability of natural convection in a vertical slot, *J. Fluid Mech.* **36,** 1–25 (1969).
12. S. A. Korpela, D. Gözüm and C. B. Baxi, On the stability of the conduction regime in a vertical slot, *Int. J. Heat Mass Transfer* **16,** 1683–1690 (1973).
13. R. V. Birikh, G. Z. Gershuni, E. M. Zhukhovitskii and R. N. Rudakov, Hydrodynamic and thermal instability of steady convective flow, *P.M.M.* **32**(2), 246–252 (1968).
14. G. Z. Gershuni and E. M. Zukhovitskii, Stability of plane parallel convective motion with respect to spatial perturbations, *P.M.M.* **33,** 830–835 (1969).
15. S. F. Liang and A. Acrivos, Stability of buoyancy-driven convection in a tilted slot, *Int. J. Heat Mass Transfer* **13,** 449–458 (1970).
16. U. H. Kurzweg, Stability of natural convection within an

inclined channel, *J. Heat Transfer, Trans. ASME* **14**, 190–191 (1970).
17. J. Hart, Stability of the flow in a differentially heated inclined box, *J. Fluid Mechanics* **47**, 547–576 (1970).
18. S. A. Korpela, A study on the effect of Prandtl number on the stability of the conduction regime of natural convection in an inclined slot, *Int. J. Heat Mass Transfer* **17**, 215–222 (1974).
19. Y. Bayazitoğlu and Y. O. Bayazitoğlu, The stability of conduction regime of combined buoyancy mode driven flow in a slot, *Lett. Appl. Engng Sci.* **5**, 259–272 (1977).
20. M. A. Hassab and M. N. Özişik, Effects of radiation and convective boundary conditions on the stability of fluid in an inclined slender slot, *Int. J. Heat Mass Transfer* **1**, 1095–1106 (1979).
21. M. N. Özişik and M. A. Hassab, Effects of convective boundary conditions on the stability of conduction regime in an inclined slender slot, *Int. J. Numerical Heat Transfer* **2**, 251–260 (1979).

APPENDIX

Principle of exchange of stabilities

It can be proved from the eigenvalue system defined by equations (1), (3) and (4) that, the instability sets in as stationary cells and not as overstability. The procedure for such an analysis can be outlined by following the pattern established in reference [5]. That is, equations (1a), (1b) and (3a) and (3b) for $a_i = a_2$ are multiplied by the complex conjugates of v^*, θ^*, θ_1^* and θ_2^*, respectively. Integrating over the entire range of the y-variable, and after some partial integrations and manipulations the following variational problem is obtained

$$(-D\bar{\theta})a_2^2 Ra_e \cdot \cos\delta = \frac{\theta^0 + \sum_{i=0}^{2}\int_i^{c_i}[D\theta_i^* D\tilde{\theta}_i^* + (a_2^2 + \tilde{c}Pr\gamma_i)\theta_i^*\tilde{\theta}_i^*]\,dy}{\int_0^1 [D^2 v^* D^2\tilde{v}^* + (2a_2^2+c)Dv^* D\tilde{v}^* + a_2^2(a_2^2+c)v^*\tilde{v}^*]\,dy} \quad (29)$$

where

$$\theta^0 = [\kappa_{w1}H_{w1}\theta_1^*(-s_1)\tilde{\theta}_1^*(-s_1) + \kappa_{w2}H_{w2}\theta_2^*(1+s_2)\tilde{\theta}_2^*(1+s_2)] \quad (30)$$

and $\tilde{}$ denotes the complex conjugate, with

$$\theta_i^* = \theta^*, \quad \gamma_i = 1 \quad \text{for } i = 0$$
$$b_i = 0, \quad c_i = 1 \quad \text{for } i = 0$$
$$b_i = -s_1, \quad c_i = 0 \quad \text{for } i = 1$$
$$b_i = 1, \quad c_i = 1 + s_2 \quad \text{for } i = 2.$$

Now, we let $c = c_r + ic_{im}$, and equate the imaginary parts on each side of equation (11); the resulting expression implies that for $(-D\theta)\cdot Re_e \cdot \cos\delta > 0$, the imaginary part of c, $c_{im} = 0$. This conclusion establishes the principle of exchange of stabilities. Namely, if the fluid is heated from below, the marginal state of instability for this system is characterized by $c = 0$ for inclinations from the horizontal such that $\delta < 90°$.

EFFETS DE LA RESISTANCE THERMIQUE PARIETALE SUR LA STABILITE D'UN REGIME DE CONDUCTION DANS UNE FENTE ETROITE ET INCLINEE

Résumé—On étudie analytiquement les effets de la résistance thermique pariétale sur l'apparition du mouvement de convection cellulaire dans un fluide à l'intérieur d'une fente inclinée, ayant un très grand allongement et soumise à des conditions aux limites convectives; des calculs numériques sont effectués dans le cas $Pr = 0{,}72$. Pour établir le domaine de validité d'une analyse déjà utilisée antérieurement pour les effets des parois sur la stabilité, les résultats présents sont comparés avec ceux obtenus par cette analyse. On étudie les effets des parois sur l'analyse de transition entre les rouleaux longitudinaux et les rouleaux transversaux.

EINFLÜSSE DES THERMISCHEN WANDWIDERSTANDS AUF DIE STABILITÄT DES ZUSTANDES DER REINEN WÄRMELEITUNG IN EINEM SCHRÄGEN SCHMALEN SPALT

Zusammenfassung—Die Einflüss des thermischen Wandwiderstands auf das Einsetzen der zellenförmigen Konvektionsbewegung in einem Fluid, das sich in einem schrägen Spalt mit großem Seitenverhältnis befindet und konvektiven Randbedingungen unterworfen ist, werden bezüglich der Längs- und Querwalzen analytisch und numerisch für den Fall $Pr = 0{,}72$ untersucht. Um den Gültigkeitsbereich der Methode der konzentrierten Parameter festzustellen, die in einigen vorangegangenen Arbeiten über die Einflüsse der Wände auf die Stabilitätskriterien verwendet wurde, werden die vorliegenden Ergebnisse mit jenen verglichen, die mit der Methode der konzentrierten Parameter erhalten wurden. Es wird gezeigt, daß die auf der Methode der konzentrierten Parameter basierenden Ergebnisse unrealistisch sind, wenn die Wärmeleitfähigkeit und die Dicke der Wände etwa in der gleichen Großenordnung liegen oder größer als die des Fluids sind. Die Einflüsse der Wände auf den Übergangswinkel für den Umschlag von Längs- zu Querwalzen wurden untersucht.

ВЛИЯНИЕ ТЕРМИЧЕСКОГО СОПРОТИВЛЕНИЯ СТЕНКИ НА УСТОЙЧИВОСТЬ РЕЖИМА ТЕПЛОПРОВОДНОСТИ В НАКЛОННОЙ УЗКОЙ ЩЕЛИ

Аннотация — Аналитически исследуется влияние термического сопротивления стенки на возникновение ячеистой конвекции в жидкости, заключенной внутри наклонной щелевой полости с очень большим отношением сторон при условиях, когда имеют место продольные и поперечные валы. Выполнены численные расчеты для $Pr = 0{,}72$. Для установления области применимости анализа на основе рассмотрения явления как системы со сосредоточенными параметрами, применявшегося в ряде ранее проведенных исследований влияния стенок на критерии устойчивости, проведено сравнение результатов этого анализа с полученными в настоящей работе. Показано, что если порядок величин теплопроводности и толщины стенок тот же, что и теплопроводности и толщины слоя жидкости, результаты анализа на основе обобщенного параметра оказываются неверными. Исследуется влияние стенок на угол наклона щели, при котором происходит переход от продольных к поперечным валам.